

Some Recent Results from LHCb

Michael D. Sokoloff

University of Cincinnati
on behalf of the LHCb Collaboration

August 24, 2016

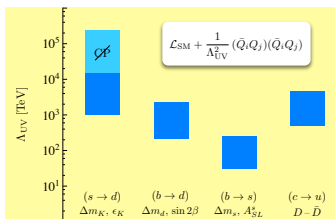
Why Flavor Physics?

- Search for manifestations of **New Physics at the highest energy scales** by studying rare and forbidden decays and searching for CP violation beyond that described by the Kobayashi-Maskawa phase of the CKM matrix.
 - CP violation in D^0 mixing
 - CP violation in B_s mixing
 - direct CP violation in four-body Λ_b decay
- Better understand strong interactions in the **Standard Model**, especially its non-perturbative aspects.
 - study $K^{*+} \rightarrow \phi K^+$ and $X^0 \rightarrow J/\psi \phi$ structures in $B^+ \rightarrow J/\psi \phi K^+$
 - study character of $Z(4430)^-$ observed in $B^0 \rightarrow \psi(2S)K^+\pi^-$
- Use cross-section measurements to probe the structure of the proton
- Probe the “hidden sector” searching for rare decays producing low mass particles with very small couplings to ordinary matter.

Flavor Constrains BSM Physics

Operator	Bounds on Λ in TeV ($c_{NP} = 1$)		Bounds on c_{NP} ($\Lambda = 1$ TeV)		Observables
	Re	Im	Re	Im	
$(\bar{s}_L \gamma^\mu d_L)^2$	9.8×10^2	1.6×10^4	9.0×10^{-7}	3.4×10^{-9}	$\Delta m_K; \epsilon_K$
$(\bar{s}_R d_L)(\bar{s}_L d_R)$	1.8×10^4	3.2×10^5	6.9×10^{-9}	2.6×10^{-11}	
$(\bar{c}_L \gamma^\mu u_L)^2$	1.2×10^3	2.9×10^3	5.6×10^{-7}	1.0×10^{-7}	$\Delta m_D; q/p _D, \phi_D$
$(\bar{c}_R u_L)(\bar{c}_L u_R)$	6.2×10^3	1.5×10^4	5.7×10^{-8}	1.1×10^{-8}	
$(\bar{b}_L \gamma^\mu d_L)^2$	6.6×10^2	9.3×10^2	2.3×10^{-6}	1.1×10^{-6}	$\Delta m_{B_d}; \sin(2\beta)$ from $B_d \rightarrow \psi K$
$(\bar{b}_R d_L)(\bar{b}_L d_R)$	2.5×10^3	3.6×10^3	3.9×10^{-7}	1.9×10^{-7}	
$(\bar{b}_L \gamma^\mu s_L)^2$	1.4×10^2	2.5×10^2	5.0×10^{-5}	1.7×10^{-5}	$\Delta m_{B_s}; \sin(\phi_s)$ from $B_s \rightarrow \psi \phi$
$(\bar{b}_R s_L)(\bar{b}_L s_R)$	4.8×10^2	8.3×10^2	8.8×10^{-6}	2.9×10^{-6}	

Flavor Structure in the SM and Beyond



Generic bounds without a flavor symmetry

- Table above from Isidori and Teubert, Eur.Phys.J.Plus **129**, 40 (2014). Bounds on representative dimension-six $\Delta F = 2$ operators.
- Image to the left from M. Neubert, EPS-HEP-2011.

No-So-Exotic Hadrons

A SCHEMATIC MODEL OF BARYONS AND MESONS *

M. GELL-MANN

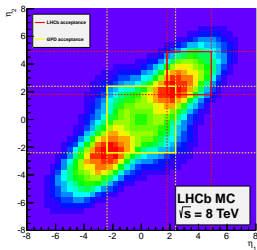
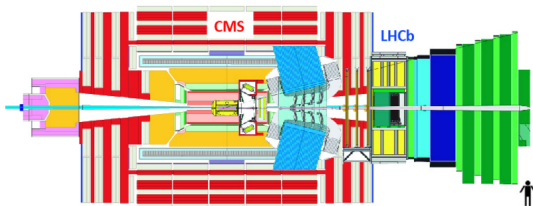
California Institute of Technology, Pasadena, California

Received 4 January 1964

Gell-Mann's original discussion of hadron properties in terms of quarks also *explicitly* suggested tetra-quark states ($qq\bar{q}\bar{q}$) and penta-quark state ($qqqq\bar{q}$) as well as "ordinary" mesons ($q\bar{q}$) and baryons (qqq).

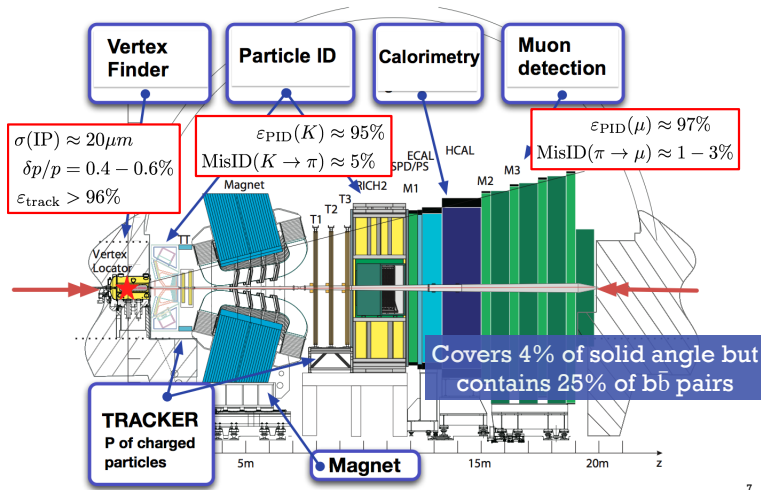
A simpler and more elegant scheme can be constructed if we allow non-integral values for the charges. We can dispense entirely with the basic baryon b if we assign to the triplet t the following properties: spin $\frac{1}{2}$, $z = -\frac{1}{3}$, and baryon number $\frac{1}{3}$. We then refer to the members $u^{\frac{2}{3}}$, $d^{-\frac{1}{3}}$, and $s^{-\frac{1}{3}}$ of the triplet as "quarks" q and the members of the anti-triplet as anti-quarks \bar{q} . Baryons can now be constructed from quarks by using the combinations (qqq), ($qqq\bar{q}\bar{q}$), etc., while mesons are made out of ($q\bar{q}$), ($q\bar{q}\bar{q}\bar{q}$), etc. It is assumed that the lowest baryon configuration (qqq) gives just the representations **1**, **8**, and **10** that have been observed, while the lowest meson configuration ($q\bar{q}$) similarly gives just **1** and **8**.

LHC Detector Acceptances for $b\bar{b}$ Production

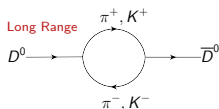
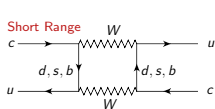


- LHCb is a forward spectrometer, optimized for accepting both B and \bar{B} hadrons in an event;
- accepts about $10\times$ as many triggers as ATLAS or CMS;
- $\sigma(c\bar{c}) \sim 20 \times \sigma(b\bar{b})$;
- acceptance in η complements ATLAS and CMS for many electro-weak studies.

LHCb Detector [2008 JINST 3 S08005]



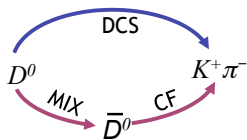
Neutral Meson Oscillation and CP Violation in Mixing



$$|P_{1,2}\rangle = p|P^0\rangle \pm q|\bar{P}^0\rangle; \quad p^2 + q^2 = 1$$

$$x \equiv \frac{\Delta m}{\Gamma} \quad y \equiv \frac{\Delta\Gamma}{2\Gamma}$$

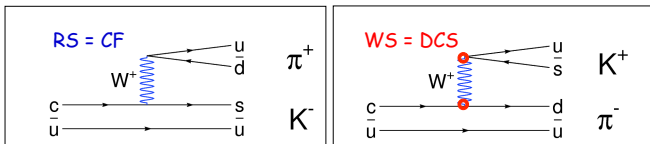
$$|\mathcal{M}|^2 \propto \frac{1}{2} e^{-\Gamma t} \left\{ |\mathcal{A}_\alpha|^2 \left(\cosh y \Gamma t + \cos x \Gamma t \right) + |\bar{\mathcal{A}}_\alpha|^2 \left| \frac{q}{p} \right|^2 \left(\cosh y \Gamma t - \cos x \Gamma t \right) + 2 \left[\Re \left(\left(\frac{q}{p} \right)^* \mathcal{A}_\alpha \bar{\mathcal{A}}_\alpha^* \right) \sinh y \Gamma t - \Im \left(\left(\frac{q}{p} \right)^* \mathcal{A}_\alpha \bar{\mathcal{A}}_\alpha^* \right) \sin x \Gamma t \right] \right\}.$$



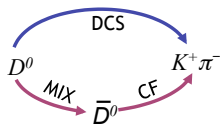
for $x, y \ll 1$ (valid for D^0 , not for B_s):

- doubly Cabibbo-Suppressed (DCS) $\approx \propto e^{-\Gamma t}$;
- pure mixing $\propto e^{-\Gamma t} \times (\Gamma t)^2$
- interference $\approx \propto e^{-\Gamma t} \times \Gamma t$

Time Evolution of $D^0 \rightarrow K\pi$



DCS and mixing amplitudes interfere to give a "quadratic" WS decay rate ($x, y \ll 1$):

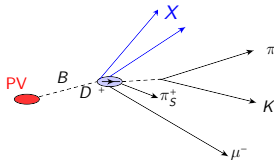
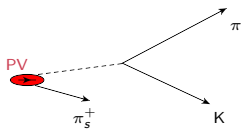


$$\frac{\Gamma_{WS}(t)}{e^{-t/\tau}} \propto R_D + \sqrt{R_D} y' \left(\frac{t}{\tau}\right) + \left(\frac{x'^2 + y'^2}{4}\right) \left(\frac{t}{\tau}\right)^2$$

where $x' = x \cos \delta + y \sin \delta$ $y' = y \cos \delta - x \sin \delta$
 and δ is the phase difference between DCS and CF decays.

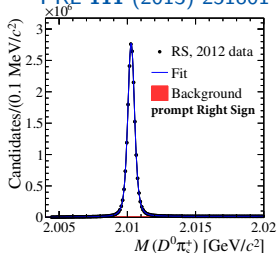
$$m_i, \Gamma_i \Leftrightarrow \text{weak eigenstates}; \quad x \equiv \frac{\Delta m}{\langle \Gamma \rangle}; \quad y \equiv \frac{\Delta m}{2 \langle \Gamma \rangle}; \quad \tau \equiv \frac{1}{\langle \Gamma \rangle}$$

$D^0 \rightarrow K\pi$ Samples: Prompt and Doubly-Tagged (DT)

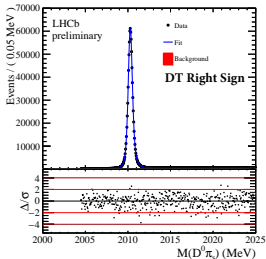


- prompt signal trigger becomes “fully” efficient well above one lifetime;
- doubly-tagged trigger is \sim independent of D^0 decay time;

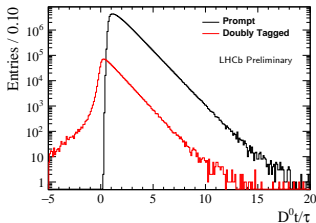
PRL 111 (2013) 251801



LHCb-PAPER-2016-033



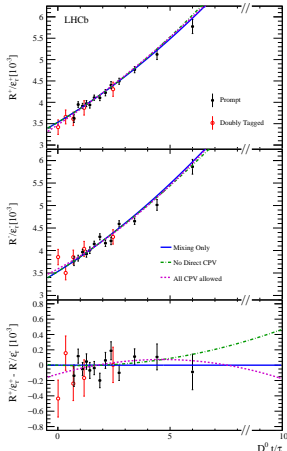
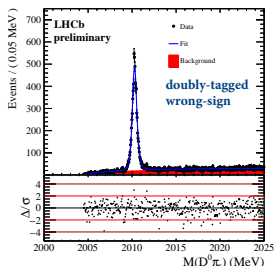
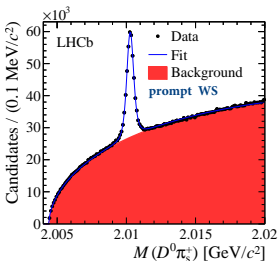
LHCb-PAPER-2016-033



$D^0 \rightarrow K\pi$ Mixing and CPV Measurements

$$R^\pm(t) = \frac{WS(t)}{RS(t)} = R_D^\pm + \sqrt{R_D^\pm} y' \left(\frac{t}{\tau}\right) + \left(\frac{x'^{\pm 2} + y'^{\pm 2}}{4}\right) \left(\frac{t}{\tau}\right)^2$$

PRL 111 (2013) 251801; LHCb-PAPER-2016-033

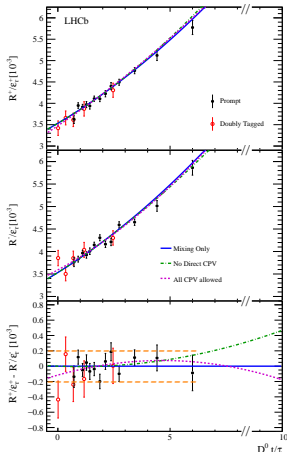
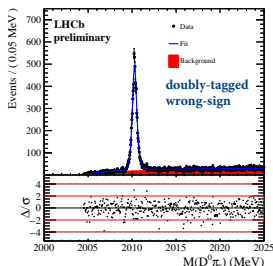
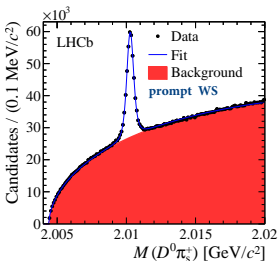


- ~ 54 M prompt RS, ~ 1.7 M DT RS;
- ~ 230 K WS, ~ 6 K WS DT;
- D^0, \bar{D}^0 mixing rates are equal, $\pm 5\%$.
- adding DT sample [$\mathcal{O}(3\%)$] improves precision by (10 – 20)%.

$D^0 \rightarrow K\pi$ Mixing and CPV Measurements

$$R^\pm(t) = \frac{WS(t)}{RS(t)} = R_D^\pm + \sqrt{R_D^\pm} y' \left(\frac{t}{\tau}\right) + \left(\frac{x'^{\pm 2} + y'^{\pm 2}}{4}\right) \left(\frac{t}{\tau}\right)^2$$

PRL 111 (2013) 251801; LHCb-PAPER-2016-033



- ~ 54 M prompt RS, ~ 1.7 M DT RS;
- ~ 230 K WS, ~ 6 K WS DT;
- D^0, \bar{D}^0 mixing rates are equal, $\pm 5\%$.
- adding DT sample [$\mathcal{O}(3\%)$] improves precision by (10 – 20)%.

Phenomenology of B_s Mixing and CP Violation

In the special case when the B_s decays semi-leptonically ($\bar{B}_s \rightarrow D_s^+ \mu^- X$), there is no DCS amplitude. Thus, the WS rate results from pure mixing.

$$|\mathcal{M}|^2 \propto \frac{1}{2} e^{-\Gamma t} \left\{ |\bar{\mathcal{A}}_\alpha|^2 \left| \frac{q}{p} \right|^2 \left(\cosh y \Gamma t - \cos x \Gamma t \right) \right\}$$

The difference in mixing rates for $B_s \rightarrow \bar{B}_s$ and $\bar{B}_s \rightarrow B_s$ (as $p \neq q$) produces an asymmetry in the rates to these final states:

$$a_{\text{sl}} \equiv \frac{\Gamma(\bar{B}_s \rightarrow f) - \Gamma(B_s \rightarrow \bar{f})}{\Gamma(\bar{B}_s \rightarrow f) + \Gamma(B_s \rightarrow \bar{f})} \approx \frac{\Delta\Gamma_s}{\Delta m_s} \tan \phi_{12s} ,$$

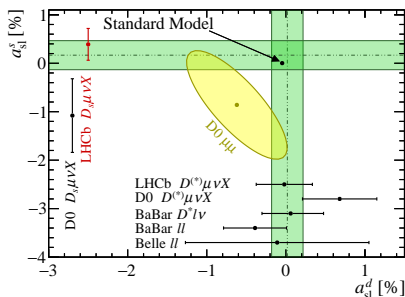
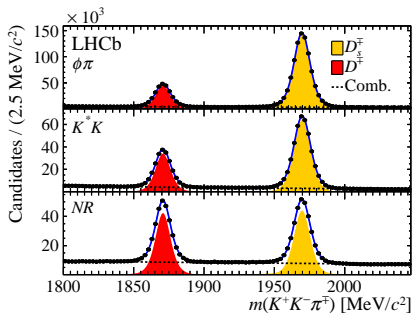
Here, $x_s \equiv \Delta m_s / \Gamma_s \gg 1$ while $y_s \equiv \Delta\Gamma_s / 2\Gamma_s \ll x_s$. As a result, the mixing period is much less than the lifetime. Tagging the flavor of a B_s when it is produced is not efficient, and measuring the time-integrated asymmetry introduces only a factor of 2 dilution in sensitivity. Hence, a_{sl}^s is calculated as

$$a_{\text{sl}}^s = \frac{2}{1 - f_{\text{bkg}}} (A_{\text{raw}} - A_{\text{det}} - f_{\text{bkg}} A_{\text{bkg}}) ,$$

where A_{det} is the detection asymmetry, f_{bkg} is the fraction of b -hadron background and A_{bkg} the background asymmetry.

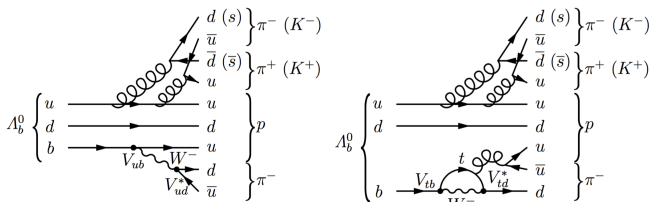
CP Violation in B_s Mixing

PRL 117 (2016) 061803

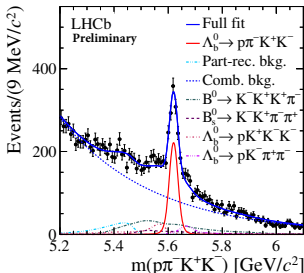
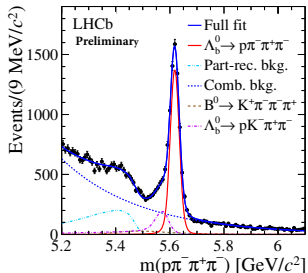


- $B_s \rightarrow D_s^\pm (\rightarrow KK\pi)\mu^\mp X$ tags flavor at decay;
- $D_s \rightarrow KK\pi$ Dalitz plot divided into three signal regions, $\phi\pi$ (900 K events), K^*K (415 K events), and non-resonant (280 K events);
- **SM** $\Rightarrow a_{sl}^s \sim 2 \times 10^{-5}$ [e.g., Lenz and Nierste, JHEP **06** (2007) 072];
- result of this analysis: $a_{sl}^s = (0.39 \pm 0.26 \pm 0.20)\%$.

$\Lambda_b^0 \rightarrow p\pi^+\pi^-\pi^-$, $\Lambda_b^0 \rightarrow p\pi^-K^+K^-$: Physics & Signals

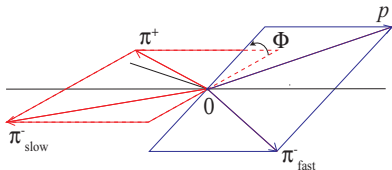


LHCb-PAPER-2016-030



Triple Product Asymmetry Math

Example: $\Lambda_b^0 \rightarrow p\pi^+\pi^-\pi^- + cc$



- $C_{\hat{T}} = \vec{p}_p \cdot (\vec{p}_{h_1^-} \times \vec{p}_{h_2^+}) [\Lambda_b^0]$
- $\bar{C}_{\hat{T}} = \vec{p}_{\bar{p}} \cdot (\vec{p}_{h_1^+} \times \vec{p}_{h_2^-}) [\bar{\Lambda}_b^0]$

$$A_{\hat{T}}(C_{\hat{T}}) = \frac{N(C_{\hat{T}} > 0) - N(C_{\hat{T}} < 0)}{N(C_{\hat{T}} > 0) + N(C_{\hat{T}} < 0)}$$

$$\bar{A}_{\hat{T}}(\bar{C}_{\hat{T}}) = \frac{\bar{N}(-\bar{C}_{\hat{T}} > 0) - \bar{N}(-\bar{C}_{\hat{T}} < 0)}{\bar{N}(-\bar{C}_{\hat{T}} > 0) + \bar{N}(-\bar{C}_{\hat{T}} < 0)}$$

$$a_P^{\hat{T}\text{-odd}} = \frac{1}{2} (A_{\hat{T}} + \bar{A}_{\hat{T}})$$

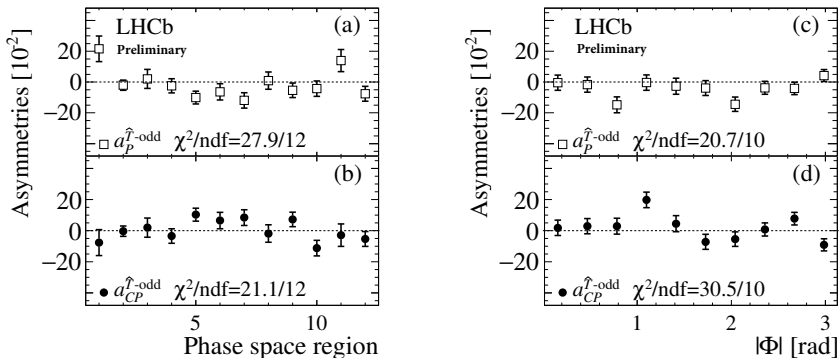
$$a_{CP}^{\hat{T}\text{-odd}} = \frac{1}{2} (A_{\hat{T}} - \bar{A}_{\hat{T}})$$

$\Lambda_b^0 \rightarrow p\pi^+\pi^-\pi^-$ and $\Lambda_b^0 \rightarrow p\pi^-K^+K^-$ TPAs

- $\approx 6000 \Lambda_b^0 \rightarrow p\pi^+\pi^-\pi^-$ and $\approx 1000 \Lambda_b^0 \rightarrow p\pi^-K^+K^-$ studied;
- **Analysis performed blindly.** All event selection criteria *and* all analysis procedures (including division of phase space into bins, defining statistical procedure to be employed, etc.) determined prior to examining data; similarly, all systematic uncertainties were evaluated prior to examining (unblinded) data.
- **globally**, no significant parity or *CP* violation observed in either sample;
- two binning schemes employed; one separates the data into disjoint subsamples according to two-body invariant masses and azimuthal angle; the other separates the data into disjoint samples using only azimuthal angle.
- **locally**, no significant parity or *CP* violation in $\Lambda_b^0 \rightarrow p\pi^-K^+K^-$.

Evidence for parity and CP violation in $\Lambda_b^0 \rightarrow p\pi^+\pi^-\pi^-$

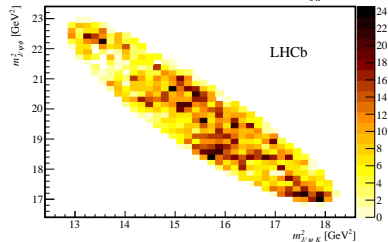
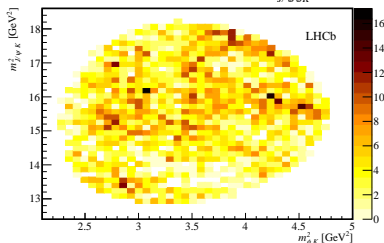
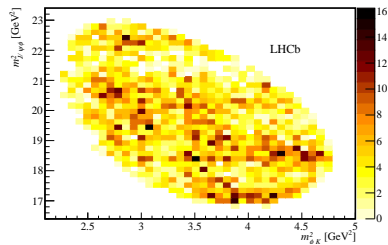
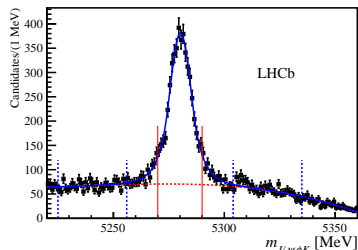
LHCb-PAPER-2016-030, in preparation



- The consistency of the data with the CP symmetry hypothesis is found to be $p = 9.8 \times 10^{-4}$ (3.3σ) using a well-established statistical test (R. A. Fisher, *The Design of Experiments* 1935), employing pseudoexperiments based on permuting the real data events to capture correlations.

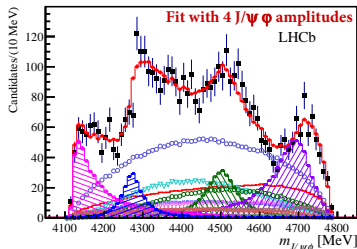
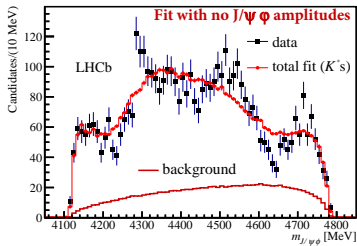
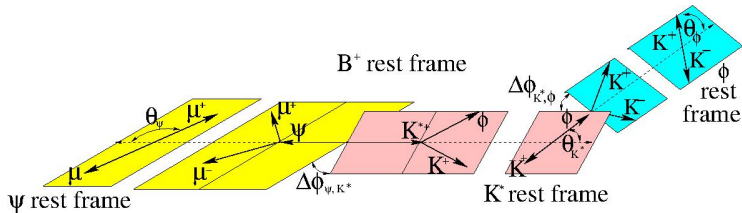
Structure in $B^+ \rightarrow J/\psi\phi K^+$ LHCb-PAPER-2016-018 & 2016-019

Dalitz plot distributions are background-subtracted and efficiency-corrected



Some Fit Projections for $B^+ \rightarrow J/\psi\phi K^+$

LHCb-PAPER-2016-018 & LHCb-PAPER-2016-019



$J/\psi \phi$ Amplitudes in the Default Fit Model

LHCb-PAPER-2016-018 & LHCb-PAPER-2016-019

Contribution	sign.	Fit results		
		M_0 [MeV]	Γ_0 [MeV]	Fit Fractions%
All $X(1^+)$				16 ± 3 $^{+6}_{-2}$
$X(4140)$	8.4σ	4146.5 ± 4.5 $^{+4.6}_{-2.8}$	83 ± 21 $^{+21}_{-14}$	13 ± 3.2 $^{+4.8}_{-2.0}$
ave. prior		4143.4 ± 1.9	15.7 ± 6.3	
$X(4274)$	6.0σ	4273.3 ± 8.3 $^{+17.2}_{-3.6}$	56 ± 11 $^{+8}_{-11}$	7.1 ± 2.5 $^{+3.5}_{-2.4}$
CDF		4274.4 $^{+8.4}_{-6.7} \pm 1.9$	32 $^{+22}_{-15} \pm 8$	
CMS		$4313.8 \pm 5.3 \pm 7.3$	38 $^{+30}_{-15} \pm 16$	
All $X(0^+)$				28 ± 5 $^{+7}_{-7}$
NR $J/\psi \phi$	6.4σ			46 ± 11 $^{+11}_{-21}$
$X(4500)$	6.1σ	4506 ± 11 $^{+12}_{-15}$	92 ± 21 $^{+21}_{-20}$	6.6 ± 2.4 $^{+3.5}_{-2.3}$
$X(4700)$	5.6σ	4704 ± 10 $^{+14}_{-24}$	120 ± 31 $^{+42}_{-33}$	12 ± 5 $^{+9}_{-5}$

ave. prior see Table 1 in LHCb-PAPER-2016-019

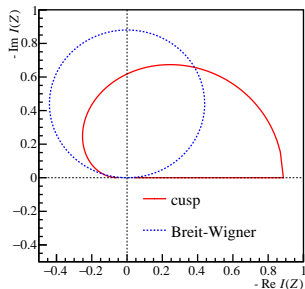
CDF arXiv:1101.6058

CMS Phys. Lett. **B734** (2014) 261

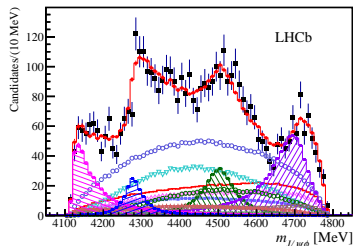
Alternative Model for $X^0(4140)$

LHCb-PAPER-2016-018 & LHCb-PAPER-2016-019

- Our 1^{++} assignment to $X(4140)$ and its large width rule out an interpretation as a 0^{++} or 2^{++} $D_s^{*+} D_s^{*-}$ molecule.
- A threshold cusp parameterization proposed by Swanson [Int. J. Mod. Phys. E **25**, no. 07, 1642010 (2016)], in which an exponential form factor, with a momentum scale (β_0) characterizes the hadron size, makes the cusp peak slightly above the sum of masses of the rescattering mesons.

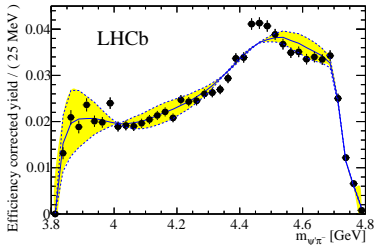
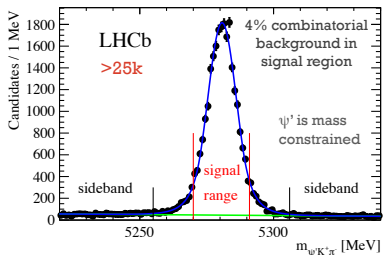


- This model fits the data as well as the default amplitude model.



$B^0 \rightarrow Z^-(4430)K^+; \quad Z^-(4330) \rightarrow \psi'\pi^-; \quad |dc\bar{c}u\rangle$

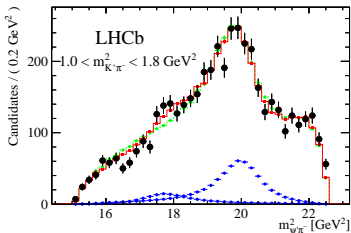
PRL 112 (2014) 222002



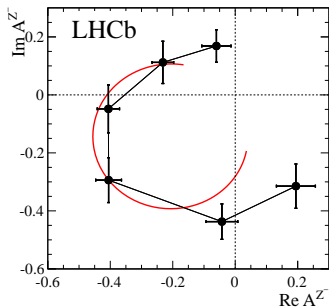
- $B^0 \rightarrow \psi' K^+ \pi^-; \quad \psi' \rightarrow \mu^- \mu^+$
- Amplitude fits plus model-independent analysis
- $Z^-(4430) \rightarrow \psi' \pi^-$ first observed by Belle [PRL 100 (2008) 142001]

- Background-subtracted, efficiency-corrected $m(\psi'\pi^-)$ distribution.
- Model projections of $\cos\theta_{K^*}$ moments up to order 4, allows for $J(K^*) \leq 2$, including correlated uncertainties.

Resonant Character of the $Z^-(4430)$



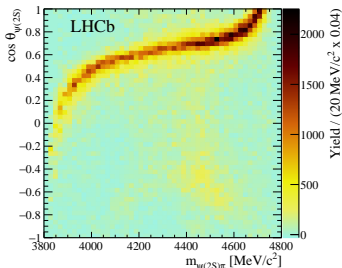
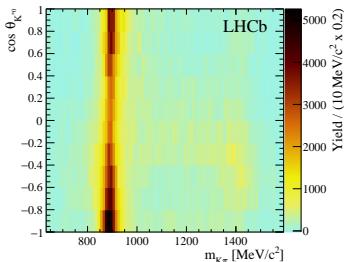
- Amplitude fit including $J^P = 1^+$ $Z^-(4430) \rightarrow \psi' \pi^-$ improves overall χ^2 corresponding to 18.7σ . [PRL 112 (2014) 222002]
- Relative to $J^P = 1^+$, the $0^-, 1^-, 2^+$, and 2^- hypotheses are rejected by at least 9.7σ , 15.8σ , 16.1σ , and 14.6σ .
- \Rightarrow **4-quark resonant state**



- A fit including an additional $J^P = 0^- \psi' \pi^-$ amplitude with $m = (4239 \pm 18^{+45}_{-10})$ MeV and $\Gamma = (220 \pm 47^{+108}_{-74})$ MeV improves overall χ^2 corresponding to 6σ .

Model-Independent Evidence for the $Z^-(4430)$ – I

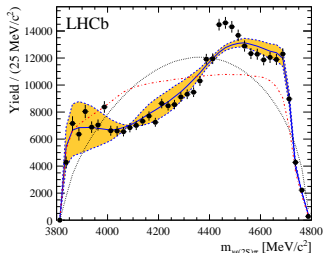
Phys. Rev. D92 (2015) 112009



- “Square Dalitz plots” expose helicity structures of amplitudes.
- The $K^*(892)$ band in the left-hand plot has two lobes produced by the $P \rightarrow VP \cos \theta$ amplitude.
- The left-hand plot also has an accumulation of events near 1400 MeV which might be produced by higher mass K^* amplitudes.
- The right-hand plot has an accumulation of events near 4430 MeV. It might be a reflection of features produced by K^* amplitudes.

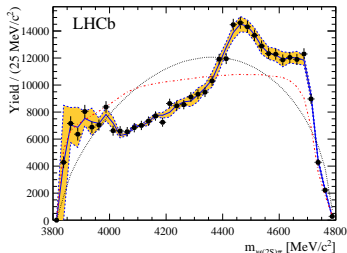
Model-Independent Evidence for the $Z^-(4430)$ – II

Phys. Rev. D92 (2015) 112009



The $\cos\theta$ distribution in each $m(K\pi)$ bin is described in terms of Legendre polynomials up to order

$$l_{\max} = \begin{cases} 2 & m(K\pi) < 836 \text{ MeV} \\ 3 & 836 \text{ MeV} < m(K\pi) < 1000 \text{ MeV} \\ 4 & m(K\pi) > 1000 \text{ MeV} . \end{cases}$$



The $\cos\theta$ distribution in each $m(K\pi)$ bin is described in terms of Legendre polynomials up to order $l_{\max} = 30$.

Using MC experiments, the $m_{\psi(2S)\pi}$ projections of the data prefer this Legendre polynomial weighting at the 15σ level.

To Take Away

- We are measuring the particle – antiparticle differences in mixing rates at the $\pm 5\%$ level in the D^0 system and at the $\pm 0.35\%$ level in the B_s system. The limits from these measurements constrain BSM physics reach at high mass scales that complement those from direct searches.
- We have observed evidence for (direct) CP violation in Λ_b decays using triple product asymmetries.
- More than 50 years after the prediction of tetra-quark and penta-quark states, we are discovering many of these in the decays of B -hadrons.
- Flavor physics is fun.